


TAZ stimulates exercise-induced muscle satellite cell activation via Pard3–p38 MAPK–TAZ signalling axis

Kyung Min Kim¹, Gi Don Yoo¹, Woong Heo¹, Ho Taek Oh¹, Jeekeon Park¹, Somin Shin¹, Youjin Do¹, Mi Gyeong Jeong², Eun Sook Hwang^{2*} & Jeong-Ho Hong^{1*} 

¹Division of Life Sciences, Korea University, Seoul, Korea; ²College of Pharmacy and Graduate School of Pharmaceutical Sciences, Ewha Womans University, Seoul, Korea

Abstract

Background Exercise stimulates the activation of muscle satellite cells, which facilitate the maintenance of stem cells and their myogenic conversion during muscle regeneration. However, the underlying mechanism is not yet fully understood. This study shows that the transcriptional co-activator with PDZ-binding motif (TAZ) stimulates muscle regeneration via satellite cell activation.

Methods *Taz*^{f/f} mice were crossed with the paired box gene 7 (*Pax7*)^{creERT2} mice to generate muscle satellite cell-specific TAZ knockout (sKO) mice. Mice were trained in an endurance exercise programme for 4 weeks. Regenerated muscles were harvested and analysed by haematoxylin and eosin staining. Muscle tissues were also analysed by immunofluorescence staining, immunoblot analysis and quantitative reverse transcription PCR (qRT-PCR). For the in vitro study, muscle satellite cells from wild-type and sKO mice were isolated and analysed. Mitochondrial DNA was quantified by qRT-PCR using primers that amplify the cyclooxygenase-2 region of mitochondrial DNA. Quiescent and activated satellite cells were stained with MitoTracker Red CMXRos to analyse mitochondria. To study the p38 mitogen-activated protein kinase (MAPK)–TAZ signalling axis, p38 MAPK was activated by introducing the MAPK kinase 6 plasmid into satellite cells and also inhibited by treatment with the p38 MAPK inhibitor, SB203580.

Results TAZ interacts with *Pax7* to induce *Myf5* expression and stimulates mammalian target of rapamycin signalling for satellite cell activation. In sKO mice, TAZ depletion reduces muscle satellite cell number by 38% (0.29 ± 0.073 vs. 0.18 ± 0.034 , $P = 0.0082$) and muscle regeneration. After muscle injury, TAZ levels (2.59-fold, $P < 0.0001$) increase in committed cells compared to self-renewing cells during asymmetric satellite cell division. Mechanistically, the polarity protein *Pard3* induces TAZ (2.01-fold, $P = 0.008$) through p38 MAPK, demonstrating that the p38 MAPK–TAZ axis is important for muscle regeneration. Physiologically, endurance exercise training induces muscle satellite cell activation and increases muscle fibre diameter (1.33-fold, 43.21 ± 23.59 vs. 57.68 ± 23.26 μm , $P = 0.0004$) with increased TAZ levels (1.76-fold, $P = 0.017$). However, sKO mice had a 39% reduction in muscle satellite cell number (0.20 ± 0.03 vs. 0.12 ± 0.02 , $P = 0.0013$) and 24% reduction in muscle fibre diameter compared to wild-type mice (61.07 ± 23.33 vs. 46.60 ± 24.29 μm , $P = 0.0006$).

Conclusions Our results demonstrate a novel mechanism of TAZ-induced satellite cell activation after muscle injury and exercise, suggesting that activation of TAZ in satellite cells may ameliorate the muscle ageing phenotype and may be an important target protein for the drug development in sarcopenia.

Keywords exercise; muscle regeneration; muscle satellite cell; sarcopenia

Received: 20 March 2023; Revised: 11 July 2023; Accepted: 11 September 2023

*Correspondence to: Jeong-Ho Hong, Division of Life Sciences, Korea University, Seoul 02841, Korea. Email: jh_hong@korea.ac.kr;
Eun Sook Hwang, College of Pharmacy, Ewha Womans University, Seoul 03760, Korea. Email: eshwang@ewha.ac.kr

Introduction

Skeletal muscle has the ability to regenerate muscle fibres after tissue damage through muscle satellite cells.^{1–3} During skeletal muscle regeneration, quiescent satellite cells are activated, which differentiate into skeletal muscle cells via the expression of muscle regulatory factors (MRFs) including MyoD, Myf5 and myogenin.^{4–7} Activated satellite cells that are not committed to differentiation undergo self-renewal to replenish the muscle stem cell pool.^{8–11} Depletion of the stem cell pool is associated with age-related muscle dysfunction.^{12,13} These studies indicate that the activation and maintenance of satellite cells are important for muscle regeneration.

Mammalian target of rapamycin (mTOR) kinase, a component of the mammalian target of rapamycin complex 1 (mTORC1), promotes anabolic processes and inhibits catabolic processes in response to nutrients, which regulate cell proliferation and organ size.¹⁴ mTORC1 is activated by the GTPase Rheb/Rheb1, which is regulated by tuberous sclerosis complex 1/2 (TSC1/2).¹⁴ Activated mTORC1 induces cellular translation through the phosphorylation of translational regulators, including ribosomal protein S6 kinase (S6K).^{14,15} It has been shown that mTOR signal is important for satellite cell activation.^{16–19}

Satellite cells are activated via asymmetric division to produce myogenic and muscle stem cells for muscle regeneration. This process facilitates their continuous production. Committed cells attached to fibres are activated to induce differentiation, but self-renewing cells unattached to fibres are converted into muscle stem cells.²⁰ During asymmetric division, the polarity protein Pard3 is predominantly localized in committed cells, compared to self-renewing cells, which induces p38 α/β mitogen-activated protein kinase (MAPK) to drive myogenesis.²¹

Exercise training has benefits to human health including improved muscle function and is a principle effector for satellite cell activation.^{22,23} Resistance exercise training facilitates muscle hypertrophy with increased satellite cell number and myonuclear expansion.^{24–27} Also, endurance exercise training activates satellite cells and stimulates muscle regeneration. Satellite cell pool enhancement was assessed with endurance exercise.^{28,29} Exercise in old mice improves muscle function. Exercise rejuvenates quiescent satellite cells,³⁰ increases satellite cell number³¹ and improves muscle regeneration in old mice.³² However, the detailed mechanism for satellite cell activation is not well understood.

Transcriptional co-regulators, transcriptional co-activator with PDZ-binding motif (TAZ) and Yes-associated protein (YAP), interact with several transcription factors to regulate cell growth and differentiation. TAZ/YAP activity is regulated by diverse extracellular signals, including Hippo, Wnt and G protein-coupled receptor (GPCR) signalling,^{33–36} which are involved in tissue homeostasis and play an important role in tis-

sue regeneration.^{37–40,51–53} It has been reported that TAZ stimulates myogenic differentiation and muscle regeneration.^{54–57} However, the mechanism underlying muscle regeneration is not yet fully understood.

In this study, we observed that TAZ stimulates muscle satellite cell activation via Pard3–p38 MAPK–TAZ signalling axis after exercise.

Materials and methods

Animals

All animal care and experimental procedures were approved by Korea University's Animal Care and Use Committee (KUIACUC-2019-0093) and were in compliance with the institutional guidelines. The mice were housed in an aseptic facility with free access to water and standard rodent chow. To generate muscle satellite cell-specific TAZ knockout (sKO) mice, *Taz*^{f/f} mice⁵⁸ with a floxed allele containing LoxP sites flanking exon 2 of *Taz* were crossed with the paired box gene 7 (*Pax7*)^{creERT2} mice. *Pax7*^{creERT2} (B6.Cg-*Pax7*^{tm1(cre/ERT2)} Gak/J, #017763) mice were purchased from the Jackson Laboratory (Bar Harbor, ME, USA). Seven-week old *Taz*^{f/f} and *Pax7*^{creERT2}:*Taz*^{f/f} mice were administered with 4-mg tamoxifen (20 mg/mL in corn oil stock solution) per 40-g body weight via intraperitoneal injection once a day for 7 days. A week later, littermate controls and experimental mice were used. Male mice aged 7–10 weeks were used in all animal studies.

Cardiotoxin-induced damage

Mice were anaesthetized with an isoflurane vaporizer, and their tibialis anterior (TA) muscles were injected with 20- μ L cardiotoxin (CTX) (0.05- μ g/ μ L stock solution, Sigma, C9759) using a 31G insulin syringe. After CTX treatment, regenerated TA muscles were harvested and analysed.

Quantification and statistical analysis

All in vivo data are presented as the mean \pm standard error of the indicated number of experimental samples. For in vitro analysis, data are represented as the mean \pm standard deviation of at least three independent experiments. Statistical significance was calculated using Student's *t* test, and the level of significance is indicated as follows: **P* < 0.05, ***P* < 0.01, ****P* < 0.001 and ns = not significant.

Data availability

This study includes no data that would need to be deposited in external repositories.

Results

Satellite cell-specific TAZ KO mice show decreased muscle regeneration after muscle damage

To study the role of TAZ in muscle regeneration, the levels of myogenic markers and TAZ were analysed during muscle regeneration after CTX-induced muscle damage. As shown in *Figure S1A*, transcription of the myogenic markers *Myf5* and *Myomaker* increased at 3, 5 and 7 days after muscle damage, respectively (3 days—*Myf5*: 4.61-fold [$P = 0.0031$] and *Myomaker*: 64.46-fold [$P = 0.0014$]/5 days—*Myf5*: 7.65-fold [$P = 0.0016$] and *Myomaker*: 140.47-fold [$P = 0.0002$]/7 days—*Myf5*: 3.34-fold [$P = 0.0076$] and *Myomaker*: 263.60-fold [$P = 0.0057$]). Additionally, the transcriptional induction of *Taz*, *Yap* and *Pax7*, a muscle satellite cell marker, was observed at 3 days after muscle damage (*Taz*: 3.75-fold [$P = 0.0034$]; *Yap*: 2.32-fold [$P = 0.0135$]; and *Pax7*: 4.85-fold [$P = 0.0036$]). Furthermore, the protein levels of TAZ, YAP and Pax7 were analysed. As shown in *Figure S1B*, TAZ was induced 1 day (3.26-fold, $P = 0.0079$) after muscle damage, and its levels significantly increased at 5 days (5.81-fold, $P = 0.0046$) after muscle damage. YAP was also induced (1 day [1.40-fold, $P = 0.0278$] and 5 days [1.72-fold, $P = 0.035$]); however, this induction was not greater than that of TAZ. Next, to study the role of TAZ in satellite cells in vivo, we developed muscle sKO mice by crossing TAZ-floxed mice (*Taz^{f/f}*) with *Pax7^{creERT2}* mice and administering tamoxifen to deplete TAZ in satellite cells (*Figure 1A*). Five days after muscle damage, wild-type (wt) and sKO mice muscles were analysed. As shown in *Figure 1B*, the sKO mice showed depleted levels of TAZ in Pax7⁺ satellite cells, as evidenced by Pax7 and TAZ immunofluorescence staining. In addition, wt mice had increased levels of TAZ, Pax7, Myf5 and embryonic myosin heavy chain (eMyHC), but the increase was not significant in the muscles of sKO mice (TAZ: wt [2.62-fold, $P = 0.001$] vs. sKO [1.18-fold, $P = 0.243$]; Pax7: wt [3.27-fold, $P = 0.0003$] vs. sKO [1.81-fold, $P = 0.0035$]; Myf5: wt [4.99-fold, $P < 0.0001$] vs. sKO [2.43-fold, $P = 0.00017$]; and eMyHC: wt [5.44-fold, $P = 0.00078$] vs. sKO [1.79-fold, $P = 0.0016$]) (*Figure 1C*). Also, wt mice showed increased *Taz*, *Pax7*, *Myf5* and *Myomaker* transcription, but this increase was not significant in sKO mice after muscle damage (*Taz*: wt [2.51-fold, $P = 0.0019$] vs. sKO [1.35-fold, $P = 0.0229$]; *Pax7*: wt [3.02-fold, $P = 0.0006$] vs. sKO [1.44-fold, $P = 0.0321$]; *Myf5*: wt [4.67-fold, $P = 0.0006$] vs. sKO [1.79-fold, $P = 0.0069$]; and *Myomaker*: wt [101.81-fold,

$P = 0.0043$] vs. sKO [46.37-fold, $P = 0.0036$]) (*Figure 1C*). Finally, the number of Pax7⁺ cells per fibre was decreased in sKO mice compared to wt mice by 38% (0.29 ± 0.073 vs. 0.18 ± 0.034 , $P = 0.0082$) (*Figure 1D*), suggesting that TAZ plays an important role in satellite cell expansion.

Next, the regeneration potential of wt and sKO mice was analysed after muscle damage. The sKO mice showed decreased levels of eMyHC by 70% (*Figure 1E*), and decreased regenerated myofibre size by 28%, as evidenced by β -dystroglycan fibre staining (*Figure 1F*). These results showed that sKO mice have impaired muscle regeneration after muscle damage, suggesting that TAZ is required by satellite cells for muscle regeneration after damage.

TAZ stimulates Myf5 transcription

Next, satellite cells from wt and sKO mice were isolated to study the role of TAZ in vitro. As shown in *Figure 2A*, TAZ-depleted satellite cells were isolated upon tamoxifen administration following CTX damage in sKO mice. These cells were incubated in satellite cell quiescence medium for 2 days and then activated in activation medium. As shown in *Figure 2B*, TAZ levels increased significantly in wt cells after activation, but this increase was not significant in sKO satellite cells (TAZ: wt [6.08-fold, $P < 0.0001$] vs. sKO [2.63-fold, $P = 0.0174$]). Pax7 levels increased in both wt and sKO satellite cells after activation, indicating that TAZ had no effect on Pax7 induction during satellite cell activation (Pax7: quiescent [$P = 0.4587$] and activated [$P = 0.3396$]) (*Figure 2B*). However, Myf5 was induced in activated wt satellite cells, but the induction was insignificant in activated sKO satellite cells (Myf5: wt [3.73-fold, $P = 0.0012$] vs. sKO [1.52-fold, $P = 0.162$]) (*Figure 2B*). Similarly, *Taz* and *Myf5* transcription increased in activated wt cells but not in activated sKO satellite cells (*Taz*: wt [1.52-fold, $P = 0.0091$] vs. sKO [1.16-fold, $P = 0.2501$]; *Myf5*: wt [1.54-fold, $P = 0.0357$] vs. sKO [1.19-fold, $P = 0.0046$]) (*Figure 2B*). *Pax7* transcription showed no difference between wt and sKO satellite cells (Pax7: quiescent [$P = 0.4543$] and activated [$P = 0.2407$]) (*Figure 2B*). In contrast, YAP knockdown in satellite cells did not alter the levels of Pax7 and Myf5 (Pax7: quiescent [$P = 0.4147$] and activated [$P = 0.4016$]; Myf5: quiescent [$P = 0.4585$] and activated [$P = 0.4891$]) (*Figure 2C*). In addition, the expression of *Pax7* and *Myf5* did not change between wt and YAP knockdown satellite cells (Pax7: quiescent [$P = 0.4543$] and activated [$P = 0.0962$]; Myf5: quiescent [$P = 0.0848$] and activated [$P = 0.5000$]) (*Figure 2C*). However, *Ctgf* and *Cyr61*, well-known target genes of YAP, were decreased in YAP knockdown satellite cells (*Ctgf*: wt [2.29-fold, $P = 0.0010$] vs. KD [1.58-fold, $P = 0.0006$]; *Cyr61*: wt [2.25-fold, $P = 0.0014$] vs. KD [1.62-fold, $P = 0.0005$]). To further examine the effect of TAZ on *Myf5* transcription, TAZ was introduced into sKO cells using TAZ-expressing adenovirus. As shown in *Figure*

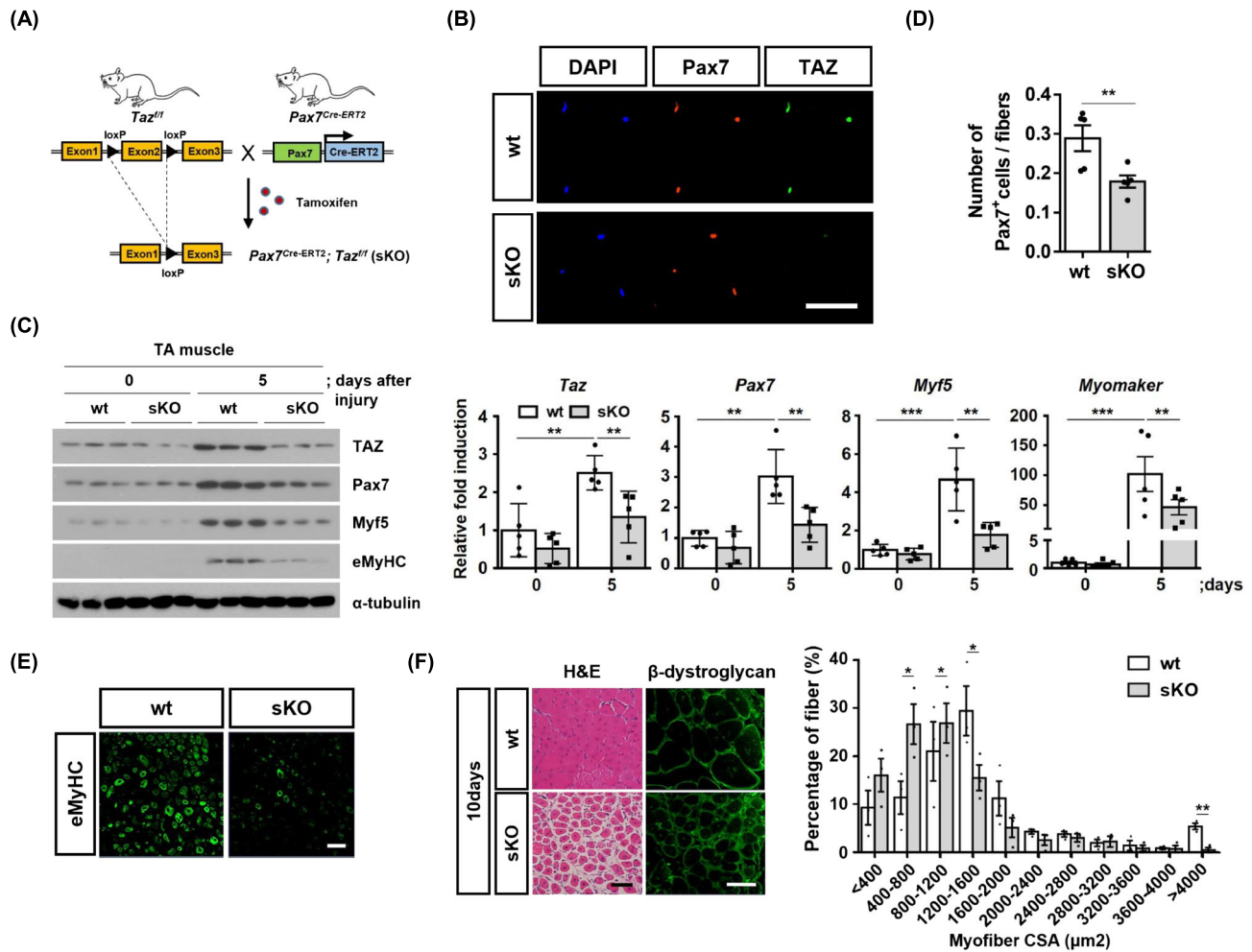


Figure 1 TAZ depletion in satellite cells impairs skeletal muscle regeneration. (A) Preparation of satellite cell-specific TAZ knockout mice (sKO). (B) Immunofluorescence staining of Pax7 (red) and TAZ (green) in tibialis anterior (TA) muscles of wt and sKO mice at 0 and 5 days after cardiotoxin (CTX) damage. The nuclei are stained with DAPI (blue). Scale bar, 50 μm. (C) Left: TAZ, Pax7, Myf5, embryonic myosin heavy chain (eMyHC) and α-tubulin levels in the TA muscles of wt and sKO mice at 0 and 5 days after CTX damage were analysed by immunoblotting. Right: the transcript levels of *Taz*, *Pax7*, *Myf5* and *Myomaker* were analysed by quantitative reverse transcription PCR in TA muscles of wt and sKO mice at 0 and 5 days after CTX damage ($n = 5$). (D) The number of Pax7-positive cells relative to the number of fibres in (B) was quantified. (E) Immunofluorescence staining of eMyHC in TA muscles of wt and sKO mice at 5 days after CTX damage. Scale bar, 50 μm. (F) Left: H&E and β-dystroglycan (green) immunofluorescence staining of TA muscles of wt and sKO mice at 10 days after CTX damage. Scale bar, 50 μm. Right: average myofiber size of TA muscles of wt and sKO mice was quantified at 10 days after CTX damage ($n = 3$). Data are presented as the mean ± SEM. * $P < 0.05$, ** $P < 0.01$ and *** $P < 0.001$ (Student's *t* test).

2D, TAZ overexpression in sKO cells restored Myf5 levels (TAZ: wt vs. sKO;Con [0.33-fold, $P = 0.0039$] and sKO;Con vs. sKO;TAZ [5.05-fold, $P = 0.0007$]; Myf5: wt vs. sKO;Con [0.30-fold, $P = 0.0026$] and sKO;Con vs. sKO;TAZ [5.60-fold, $P = 0.001$]) and *Myf5* transcription (*Taz*: wt vs. sKO;Con [0.35-fold, $P < 0.0001$] and sKO;Con vs. sKO;TAZ [4.66-fold, $P = 0.001$]; *Myf5*: wt vs. sKO;Con [0.39-fold, $P < 0.0001$] and sKO;Con vs. sKO;TAZ [3.15-fold, $P = 0.0001$]). The levels of Pax7 (Pax7: wt vs. sKO;Con [$P = 0.4179$] and sKO;Con vs. sKO;TAZ [$P = 0.2756$]) and its transcripts (*Pax7*: wt vs. sKO;Con [$P = 0.2546$] and sKO;Con vs. sKO;TAZ [$P = 0.1255$]) were not altered upon TAZ transduction (Figure 2D). These results

suggest that TAZ stimulates Myf5 transcription during satellite cell activation.

TAZ interacts with Pax7 to induce Myf5 expression

Next, we investigated whether TAZ physically interacts with Pax7. His-tagged TAZ and FLAG-tagged Pax7 expression plasmids were transfected into 293T cells, and their interaction was investigated. As shown in Figure 3A, physical interaction between TAZ and Pax7 was observed. Furthermore, an interaction between FLAG-tagged TAZ and endogenous Pax7 was

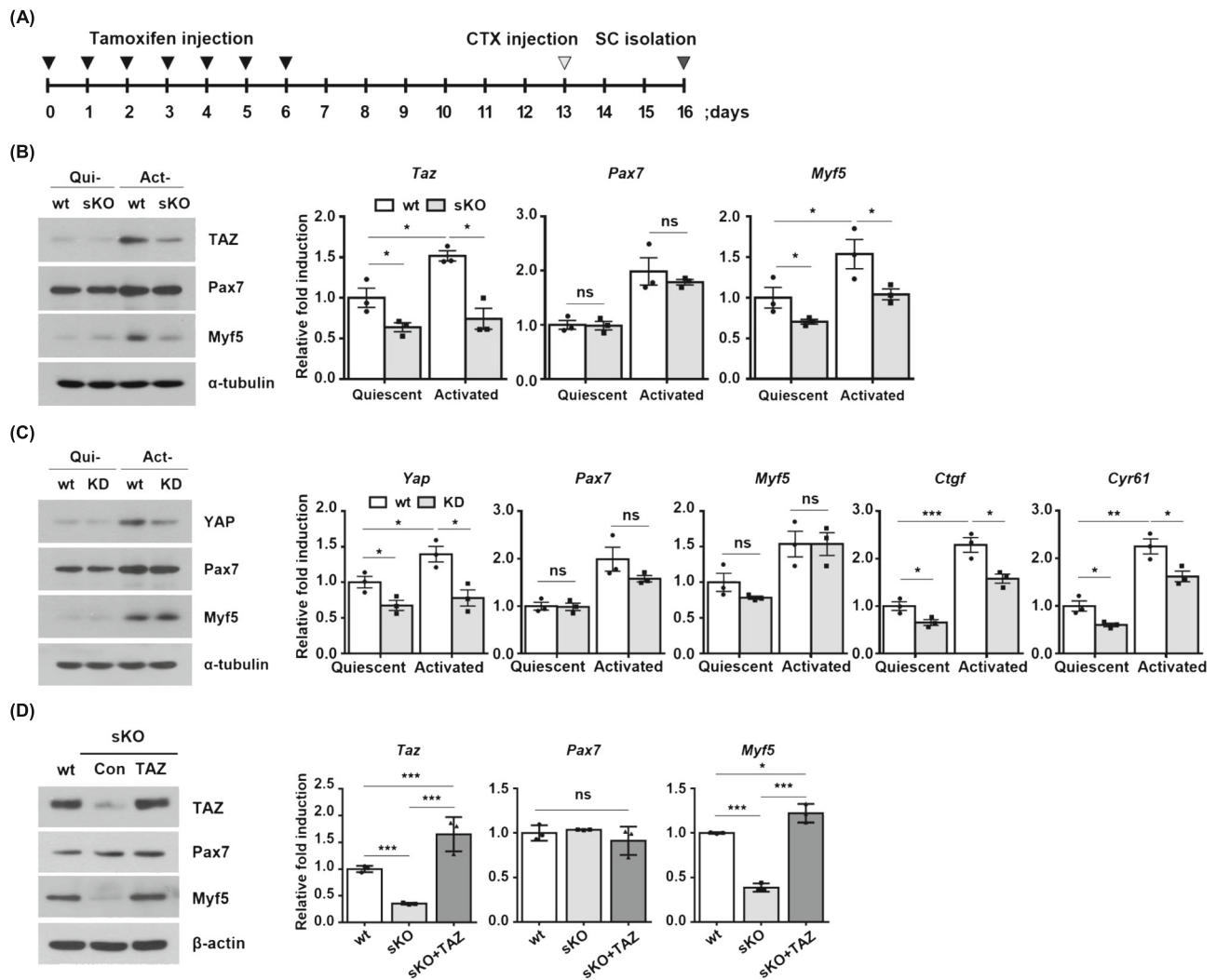


Figure 2 TAZ stimulates *Myf5* transcription, but YAP does not. (A) Experimental timeline showing time points of tamoxifen injection, cardiotoxin (CTX) injection and satellite cell isolation. (B) Left: TAZ, Pax7, Myf5 and α -tubulin levels were analysed by immunoblotting in wt and sKO satellite cells under quiescent (Qui-) and activated (Act-) culture conditions. Quiescent and activated satellite cells were prepared as described previously. Right: the transcript levels of *Taz*, *Pax7* and *Myf5* were analysed by qRT-PCR in wt and sKO satellite cells under quiescent and activated culture conditions ($n = 3$). (C) Left: YAP, Pax7, Myf5 and α -tubulin levels were analysed by immunoblotting in wt and YAP knockdown (KD) satellite cells under quiescent and activated culture conditions. Right: *Yap*, *Pax7*, *Myf5*, *Ctgf* and *Cyr61* transcription was analysed by qRT-PCR in wt and YAP knockdown satellite cells under quiescent and activated culture conditions ($n = 3$). (D) Left: TAZ, Pax7, Myf5 and β -actin levels were analysed by immunoblotting in wt, sKO and TAZ-rescued sKO satellite cells. Right: *Taz*, *Pax7* and *Myf5* transcript levels were analysed by qRT-PCR in wt, sKO and TAZ-rescued sKO satellite cells ($n = 3$). Data are presented as the mean \pm SD. * $P < 0.05$, ** $P < 0.01$ and *** $P < 0.001$ (Student's *t* test).

observed in FLAG-tagged TAZ-expressing C2C12 myoblasts (Figure 3B). We also assessed the interaction between YAP and Pax7. Interestingly, YAP did not interact with Pax7 in YAP and Pax7-overexpressing 293T cells (Figure 3A). In addition, endogenous Pax7 did not interact with YAP in YAP-overexpressing C2C12 myoblasts (Figure 3B). To determine the interaction between TAZ and Pax7, we investigated the binding domains of the interacting proteins. FLAG-tagged N-terminal- or C-terminal-deleted Pax7 expression plasmids were transfected into 293T cells along with Myc-tagged TAZ expression plasmid. Immunoprecipitation with FLAG antibodies revealed that the N-terminal region of Pax7 (amino acids

35–215) was important for its interaction with TAZ (Figure 3C), whereas the WW domain of TAZ was important for its interaction with Pax7 (Figure 3D). These results suggest that TAZ, but not YAP, regulates Pax7-mediated gene transcription and that there is a functional difference between TAZ and YAP in satellite cell activation during muscle regeneration.

Pax7 induces *Myf5* transcription during myogenic differentiation.⁵⁹ Thus, we investigated whether the interaction between TAZ and Pax7 induces *Myf5* transcription. Chromatin immunoprecipitation was performed to determine whether TAZ occupies the Pax7-binding site of the *Myf5* enhancer, located -57.5 kb from the transcription start site.⁵⁹

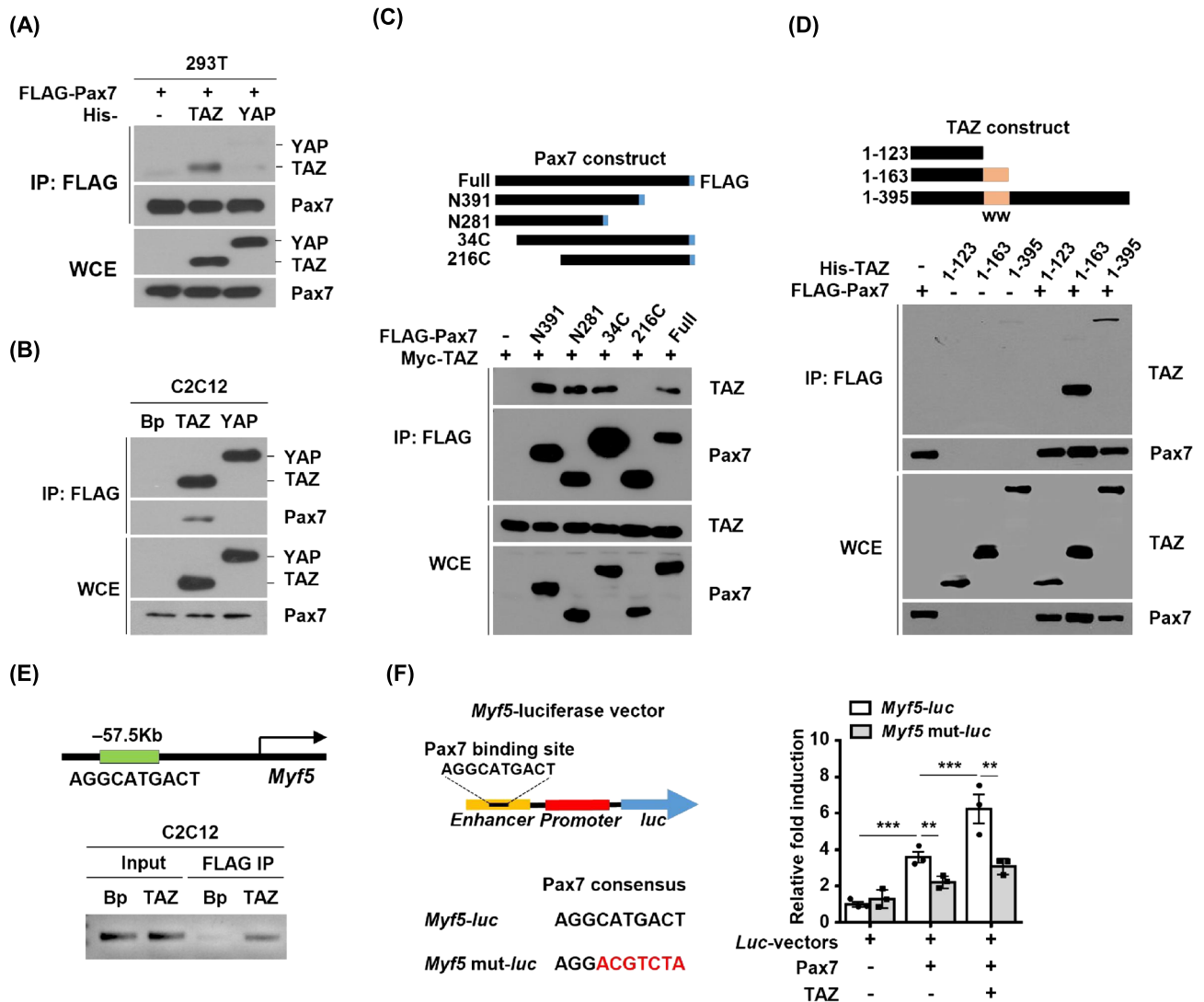


Figure 3 TAZ induces Myf5 expression by interacting with Pax7. (A) HEK293T cells were transfected with His-tagged TAZ or His-tagged YAP and FLAG-tagged Pax7 expression plasmids. After 24 h, cell lysates were immunoprecipitated using FLAG antibodies. The immunoprecipitates (IP:FLAG) and whole-cell lysates (WCE) were analysed by immunoblotting. (B) Co-immunoprecipitation analysis between endogenous Pax7 and TAZ or YAP in C2C12 cells expressing FLAG-tagged TAZ or YAP. Cell lysates were immunoprecipitated using FLAG antibodies. The immunoprecipitates and whole-cell lysates were analysed by immunoblotting. (C) Myc-tagged TAZ plasmid and FLAG-tagged Pax7 deletion constructs were transfected into HEK293T cells. After 24 h, cell lysates were immunoprecipitated using FLAG antibodies. The immunoprecipitates and whole-cell lysates were analysed by immunoblotting. (D) FLAG-tagged Pax7 plasmid and His-tagged TAZ deletion construct were transfected into HEK293T cells. After 24 h, cell lysates were immunoprecipitated using FLAG antibodies. The immunoprecipitates and whole-cell lysates were analysed by immunoblotting. (E) Chromatin immunoprecipitation was performed using control and FLAG-tagged TAZ-expressing C2C12 cells using anti-FLAG antibodies. Immunoprecipitated chromatin fragments were analysed by PCR with a primer set spanning the -57.5kb *Myf5* enhancer containing the Pax7-binding site. (F) Schematic image of *Myf5* luciferase reporter constructs containing the Pax7-binding consensus (*Myf5-luc*) or mutant (*Myf5 mut-luc*) site. HEK293T cells were transfected with *Myf5* luciferase vector, TAZ and Pax7 expression plasmids. After 24 h, luciferase activity was analysed and a *Renilla* luciferase plasmid was used to normalize transfection. Data are presented as the mean \pm SD. * $P < 0.05$, ** $P < 0.01$ and *** $P < 0.001$ (Student's *t* test).

As shown in Figure 3E, TAZ was recruited to the Pax7-binding site. To examine TAZ-mediated *Myf5* transcription, the TAZ-binding region of the *Myf5* enhancer was isolated and fused to a luciferase reporter gene (Figure 3F). When the reporter gene was co-transfected with TAZ and Pax7 expression plasmids, significant reporter gene transcription was ob-

served (Pax7 [3.60-fold, $P = 0.0007$] and Pax7 + TAZ [6.26-fold, $P = 0.0014$]) (Figure 3F). However, when the Pax7-binding site was mutated, reporter gene transcription decreased significantly (Pax7 [1.70-fold, $P = 0.0292$] and Pax7 + TAZ [2.37-fold, $P = 0.0048$]) (Figure 3F), indicating that TAZ promoted Pax7-mediated gene transcription. These re-

sults show that TAZ interacts with Pax7, which induces *Myf5* transcription, suggesting that TAZ, but not YAP, is specifically involved in Pax7-mediated gene transcription and myogenic differentiation.

TAZ activates mTOR signalling through *Rheb/Rheb1*

mTORC1 activity is necessary for the transition of satellite cells from G_0 to G_{Alert} phase.¹⁶ Activated stem cells show a dramatic increase in cell size and mitochondrial activity compared to quiescent stem cells.¹⁶ We recently reported that TAZ stimulates mitochondrial biogenesis by activating mTOR

signalling through the induction of *Rheb/Rheb1*.⁵¹⁰ Indeed, activated satellite cells showed increased levels of *Rheb*, *Rheb1*, phospho-p70 S6K (p-p70 S6K) and phospho-4E-BP (p-4E-BP) upon TAZ induction (Qui-wt vs. Act-wt: TAZ [3.70-fold, $P = 0.0016$], *Rheb* [4.35-fold, $P = 0.0012$], *Rheb1* [3.86-fold, $P = 0.0002$], p-p70 S6K [3.27-fold, $P = 0.0088$] and p-4E-BP [4.51-fold, $P = 0.0052$]) (Figure 4A). However, this increase was not observed in activated sKO satellite (Qui-sKO vs. Act-sKO: TAZ [1.97-fold, $P = 0.0131$], *Rheb* [2.01-fold, $P = 0.0128$], *Rheb1* [1.99-fold, $P = 0.0154$], p-p70 S6K [1.56-fold, $P = 0.0605$] and p-4E-BP [1.88-fold, $P = 0.1158$]) (Figure 4A). *Taz*, *Rheb* and *Rheb1* transcription was increased in activated wt satellite cells, but not in sKO satellite cells (*Taz*: wt [2.30-fold, $P = 0.00017$] vs. sKO [1.36-fold, $P = 0.0157$];

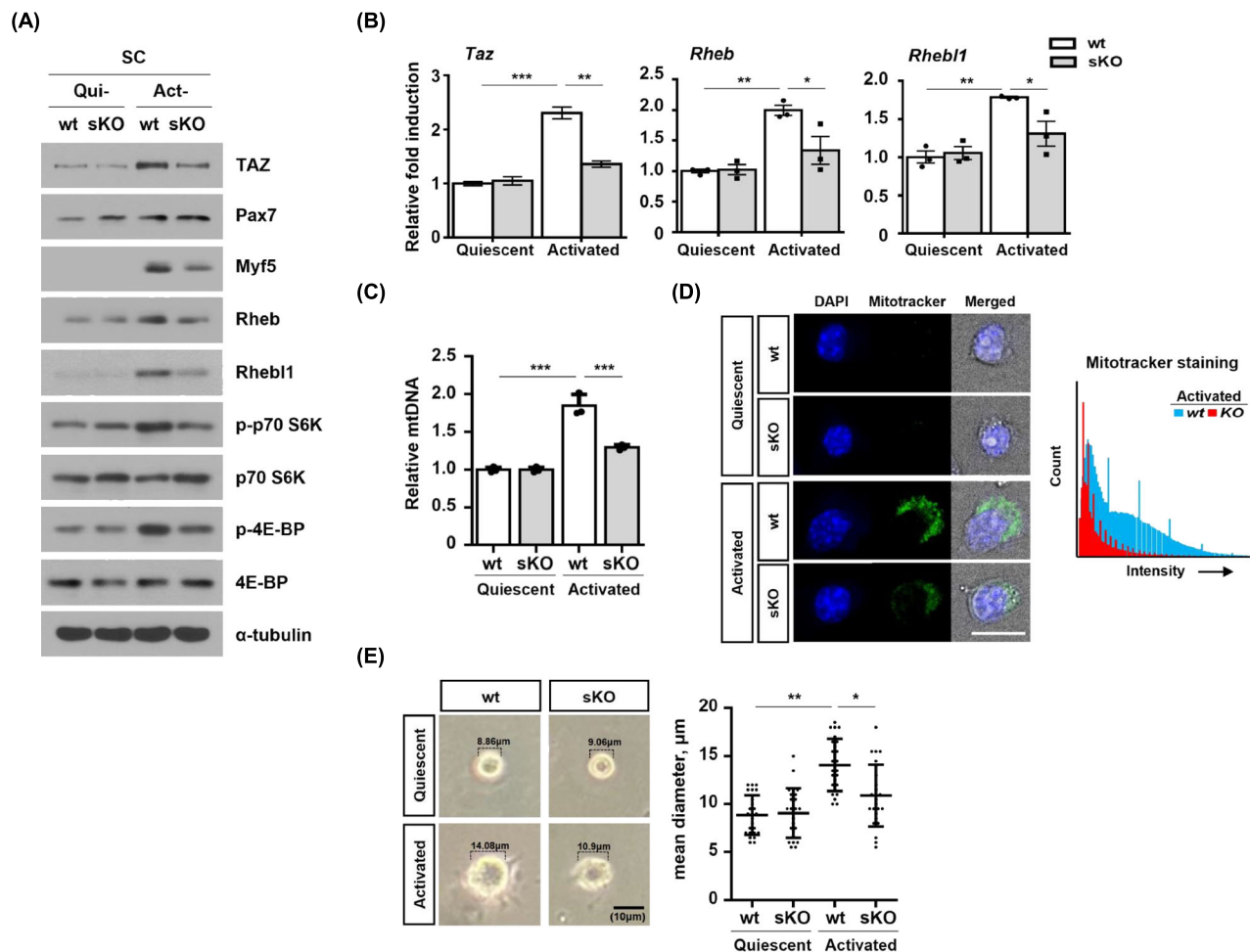


Figure 4 TAZ activates satellite cells through mTOR signalling. (A) TAZ, Pax7, Myf5, Rheb, Rheb1, phospho-p70 S6K, p70 S6K, phospho-4E-BP, 4E-BP and α -tubulin levels were analysed by immunoblotting in wt and sKO satellite cells under quiescent (Qui-) and activated (Act-) culture conditions. (B) *Taz*, *Rheb* and *Rheb1* transcript levels were analysed by qRT-PCR in wt and sKO satellite cells under quiescent and activated culture conditions ($n = 3$). (C) Mitochondrial DNA copy number was analysed by qRT-PCR using genomic DNA of wt and sKO satellite cells under quiescent and activated culture conditions ($n = 3$). (D) Wt and sKO satellite cells under quiescent and activated culture conditions were immunostained with MitoTracker to analyse the mitochondrial potential (left). The nuclei are stained with DAPI (blue). Scale bar, 10 μ m. The fluorescence intensity of each cell was quantified using ImageJ software (right). (E) Representative bright-field microscopy images of wt and sKO satellite cells under quiescent and activated culture conditions (left). The average satellite cell size was quantified using ImageJ software (right, $n = 25$). Data are presented as the mean \pm SD. * $P < 0.05$, ** $P < 0.01$ and *** $P < 0.001$ (Student's t test).

Rheb: wt [1.99-fold, $P = 0.00016$] vs. sKO [1.31-fold, $P = 0.1314$]; and *Rheb1I*: wt [1.79-fold, $P = 0.0003$] vs. sKO [1.24-fold, $P = 0.1186$] (Figure 4B). In addition, wt satellite cells showed increased mitochondrial DNA after activation (1.85-fold, $P = 0.00035$), but sKO satellite cells did not show a significant induction of mitochondrial DNA (1.29-fold, $P = 0.00027$) (Figure 4C). Increased mitochondrial potential (2.39-fold, $P = 0.0004$) was observed in activated wt satellite cells compared to sKO satellite cells, as evidenced by MitoTracker staining (Figure 4D). Finally, wt satellite cells showed increased cell size after activation (1.59-fold,

0.89 ± 0.21 vs. $1.41 \pm 0.27 \mu\text{m}$, $P < 0.0001$), but this increase was not significant in sKO satellite cells (1.20-fold, 0.91 ± 0.26 vs. $1.09 \pm 0.32 \mu\text{m}$, $P = 0.0152$) (Figure 4E). These results suggest that TAZ plays an important role in mTOR signal-mediated satellite cell activation.

TAZ is asymmetrically activated by p38 MAPK during satellite cell activation

Satellite cells are activated to produce myogenic cells from committed cells and muscle stem cells from self-renewing

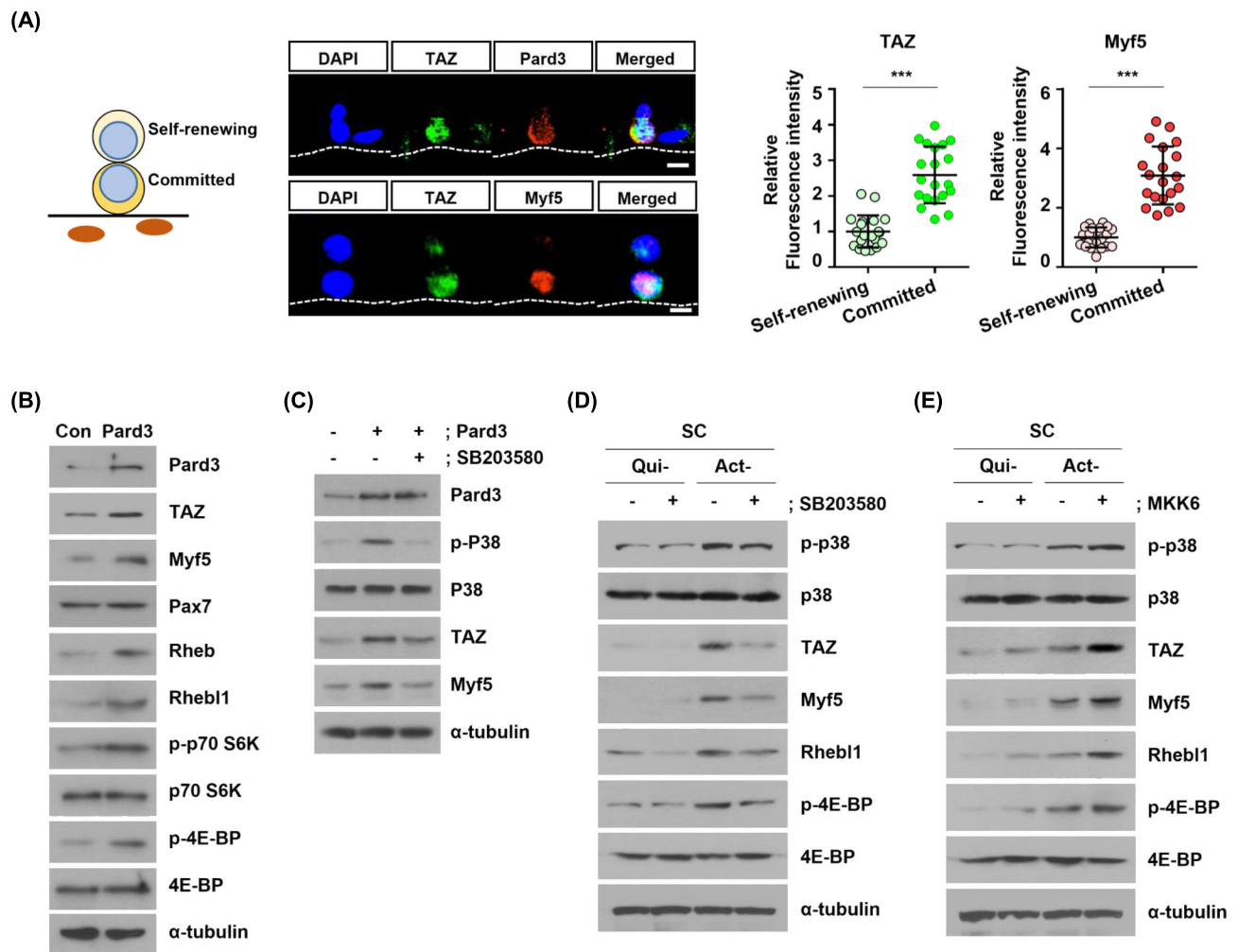


Figure 5 Pard3 increases TAZ expression in committed cells during asymmetric division of satellite cells. (A) Single extensor digitorum longus (EDL) myofibres were isolated from wt mice, and 48 h later, asymmetrically dividing satellite cells on the myofibre were immunostained for TAZ, Pard3 and Myf5. The nuclei are stained with DAPI (blue). Scale bar, 20 μm . The fluorescence intensity of TAZ and Myf5 expression in asymmetrically dividing satellite cells was quantified using ImageJ software. (B) Satellite cells were transfected with Pard3-expressing plasmid. After 24 h, Pard3, TAZ, Myf5, Pax7, Rheb, Rheb1, phospho-p70 S6K, p70 S6K, phospho-4E-BP, 4E-BP and α -tubulin levels were analysed by immunoblotting. (C) Pard3-transfected satellite cells were treated with p38 MAPK inhibitor (SB203580, 10 μM) for 24 h, and the levels of Pard3, phospho-p38, p38, TAZ, Myf5 and α -tubulin were analysed by immunoblotting. (D) Quiescent (Qui-) and activated (Act-) satellite cells were treated with SB203580 (10 μM) for 24 h, and the levels of phospho-p38, p38, TAZ, Myf5, Rheb1, phospho-4E-BP, 4E-BP and α -tubulin were analysed by immunoblotting. (E) Quiescent and activated satellite cells were transfected with MKK6 expression plasmid to activate p38 MAPK signalling. After 24 h, the levels of phospho-p38, p38, TAZ, Myf5, Rheb1, phospho-4E-BP, 4E-BP and α -tubulin were analysed by immunoblotting. Data are presented as the mean \pm SD. *** $P < 0.001$ (Student's t test).

cells through asymmetric division.²⁰ Therefore, we studied the expression and activation of TAZ during asymmetric division. As shown in *Figure 5A*, Pard3 levels were higher in committed cells than in self-renewing cells. Furthermore, TAZ and Myf5 levels were increased in committed cells (TAZ [2.59-fold, 1.00 ± 0.45 vs. 2.59 ± 0.80 , $P < 0.0001$] and Myf5 [3.09-fold, 1.00 ± 0.34 vs. 3.09 ± 0.98 , $P < 0.0001$]) (*Figure 5A*), suggesting that TAZ is induced in committed cells for the production of myogenic cells. Next, we studied whether forced Pard3 expression increased TAZ levels in satellite cells. As shown in *Figure 5B*, TAZ levels (2.01-fold, $P = 0.008$) increased in Pard3-overexpressing cells (2.90-fold, $P = 0.004$) along with increased Myf5 levels (2.22-fold, $P = 0.0008$). In addition, Pard3 induced the expression of Rheb (2.73-fold, $P < 0.0001$), Rheb1 (1.80-fold, $P = 0.0037$), p-p70 S6K (1.82-fold, $P = 0.0008$) and p-4E-BP (2.20-fold, $P = 0.0018$), indicating mTOR signal activation. These results suggest that Pard3 drives the myogenic differentiation of committed cells through TAZ activation during asymmetric division of muscle satellite cells.

Asymmetric localization of the Par complex activates p38 α/β MAPK in committed cells.²¹ To determine whether p38 MAPK stimulates TAZ, the p38 MAPK inhibitor, SB203580, was used to treat Pard3-overexpressing satellite cells. As shown in *Figure 5C*, overexpression of Pard3 (Pard3 + Con [3.52-fold, $P = 0.0049$] and Pard3 + SB [3.87-fold, $P = 0.0066$]) activated p38 MAPK (p-p38: Pard3 + Con [4.69-fold, $P = 0.0003$]), as indicated by increased phosphorylation of these proteins. However, p38 MAPK inhibitor-treated cells (p-p38: Pard3 + Con vs. Pard3 + SB [0.38-fold, $P = 0.0030$]) showed decreased TAZ levels (Pard3 + Con vs. Pard3 + SB [0.55-fold, $P = 0.0060$]) compared to control cells, suggesting that Pard3 increases TAZ expression (2.89-fold, $P = 0.0017$) through p38 MAPK activation. Next, to study whether Pard3 overexpression can promote Myf5 expression in TAZ-deficient cells, we overexpressed Pard3 in wt and sKO satellite cells to study Myf5 expression (*Figure S2*). TAZ (Con:wt vs. Pard3:wt, 3.63-fold, $P = 0.0003$) and Myf5 expression (Con:wt vs. Pard3:wt, 3.65-fold, $P = 0.0009$) was increased by Pard3 overexpression (Con:wt vs. Pard3:wt, 2.10-fold, $P = 0.0016$), but the increase was not seen in sKO satellite cells (Pard3:wt vs. Pard3:sKO, Pard3 [1.04-fold, $P = 0.3332$], TAZ [0.61-fold, $P = 0.0029$] and Myf5 [0.57-fold, $P = 0.0027$]). Thus, the results show that Pard3 increases Myf5 expression via TAZ.

Next, the effect of SB203580 was examined in quiescent and activated satellite cells. As shown in *Figure 5D*, SB203580 inhibited p38 MAPK activity (0.45-fold, $P = 0.0011$) and decreased TAZ levels (0.51-fold, $P = 0.0135$) in activated satellite cells. In addition, SB203580 decreased Myf5 (0.58-fold, $P = 0.0085$), Rheb1 (0.57-fold, $P = 0.0133$) and p-4E-BP levels (0.52-fold, $P = 0.0121$) (*Figure 5D*). In contrast, the expression of MAPK kinase 6 (MKK6), an upstream kinase of p38 MAPK, stimulated p38 MAPK activity (2.01-fold,

$P = 0.0060$) and increased TAZ levels (2.06-fold, $P = 0.0001$) in activated satellite cells. Moreover, MKK6 expression increased Myf5 (1.87-fold, $P = 0.0059$), Rheb1 (2.10-fold, $P = 0.0168$) and p-4E-BP levels (2.01-fold, $P = 0.0189$) (*Figure 5E*). These results suggest that p38 MAPK stimulates TAZ in Pard3-expressing, committed satellite cells.

TAZ stimulates both proliferation and differentiation in muscle satellite cells

To regenerate muscle after muscle injury, activated satellite cells proliferate and differentiate into myoblasts. The activity of TAZ on satellite cell proliferation and differentiation was investigated in vitro. To investigate the proliferation capacity, the protein expression of cyclin D1, a regulator of the cell cycle, was analysed in proliferating wt and sKO satellite cells. As shown in *Figure S3A*, the expression of Myf5 (0.24-fold, $P = 0.0001$) and cyclin D1 (0.25-fold, $P = 0.0021$) was decreased in sKO satellite cells compared to wt satellite cells. Cell proliferation rate was also analysed by counting the number of cells. As shown in *Figure S3B*, the cell proliferation rate (3 days: wt [2.64-fold, $P < 0.0001$] and sKO [1.74-fold, $P = 0.0001$]) was reduced in sKO satellite cells. In addition, the proliferation of wt and sKO satellite cells was analysed by fluorescence staining for Ki67, a marker of cell proliferation. As shown in *Figure S3C*, the number of Ki67⁺ cells decreased in sKO satellite cells. These results show that TAZ plays an important role in the proliferation of satellite cells.

The differentiation of wt and sKO satellite cells was also investigated by the analysing the expression of myogenic marker genes. As shown in *Figure S4A*, the reduced expression of myogenic marker genes was observed in sKO satellite cells compared to wt satellite cells (2 days [2D]: *MyoD* [0.48-fold, $P < 0.0001$] and *Myogenin* [0.47-fold, $P = 0.0032$]). In addition, as shown in *Figure S4B*, the area of MyHC⁺ expression was reduced in sKO satellite cells. These results show that TAZ plays an important role in the myogenic differentiation of satellite cells. Taken together, the results suggest that TAZ is an important factor in muscle regeneration.

TAZ stimulates satellite cell expansion and increases muscle fibre diameter after exercise

It has been shown that exercise stimulates muscle satellite cell activation and increases the satellite cell population. Indeed, after 4 weeks of exercise training, we observed that exercise training increased muscle fibre diameter (1.33-fold, 43.21 ± 23.59 vs. 57.68 ± 23.26 μm , $P = 0.0004$) as indicated by dystrophin staining (*Figure 6A*). Next, as shown in *Figure 6B*, exercise training increased the levels of Pax7 (1.52-fold, $P = 0.0387$) and Myf5 (3.86-fold, $P = 0.0022$) with an increase in the levels of TAZ (1.76-fold, $P = 0.0174$) and cyclin D1 (2.44-

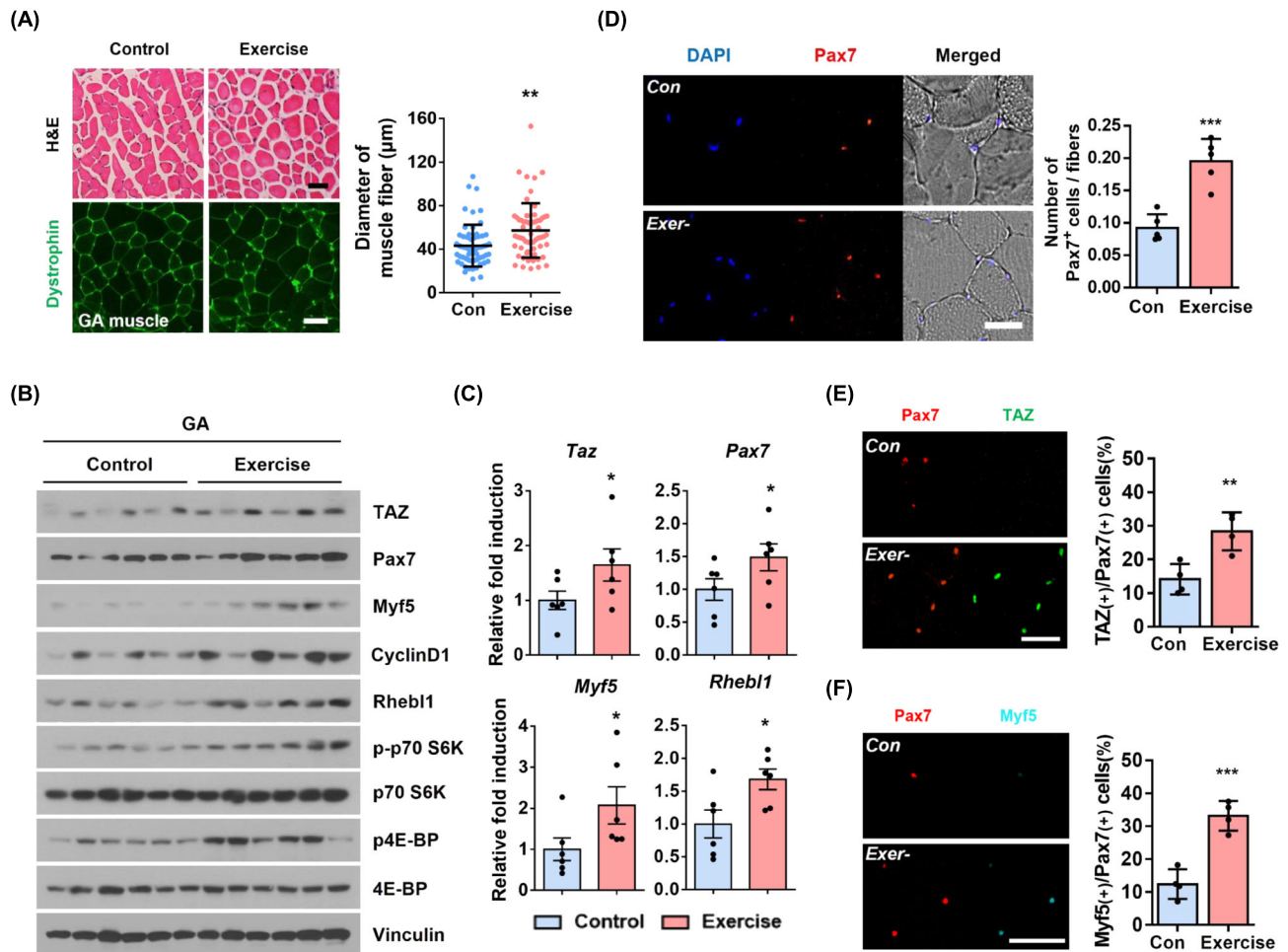


Figure 6 Exercise increases the number of satellite cells and the diameter of myofibers. (A) Wt mice were subjected to endurance exercise training. Gastrocnemius (GA) muscles were harvested from these mice, and tissue immunostaining was performed. H&E and dystrophin (green) immunofluorescence staining of GA muscles from control and exercise-trained wt mice. Scale bar, 50 μ m. Muscle fibre diameters were quantified using ImageJ software. (B) TAZ, Pax7, Myf5, Cyclin D1, Rheb1, phospho-p70 S6K, p70 S6K, phospho-4E-BP, 4E-BP and Vinculin levels in GA muscles of control and exercise-trained wt mice were analysed by immunoblotting. (C) *Taz*, *Pax7*, *Myf5* and *Rheb1* transcript levels were analysed by qRT-PCR in GA muscles of control and exercise-trained wt mice ($n = 6$). (D) Immunofluorescence staining of Pax7 (red) in GA muscles of control and exercise-trained wt mice. Nuclei are stained with DAPI (blue). Scale bar, 50 μ m. The number of Pax7-positive cells was quantified relative to the number of fibres. (E) Immunofluorescence staining of Pax7 (red) and TAZ (green) in GA muscles of control and exercise-trained wt mice. Scale bar, 50 μ m. The ratio of the number of TAZ-positive cells to the number of Pax7-positive cells was quantified. (F) Immunofluorescence staining of Pax7 (red) and Myf5 (cyan) in GA muscles of control and exercise-trained wt mice. Scale bar, 50 μ m. The ratio of the number of Myf5-positive cells to the number of Pax7-positive cells was quantified. Data are presented as the mean \pm SEM. * $P < 0.05$, ** $P < 0.01$ and *** $P < 0.001$ (Student's *t* test).

fold, $P = 0.0116$). In addition, increased mTOR activity was observed in exercise-trained mice compared to control mice. This was evidenced by increased Rheb1 (2.22-fold, $P = 0.0009$), p-p70 S6K (1.95-fold, $P = 0.0019$) and p-4E-BP (2.06-fold, $P = 0.0064$) (Figure 6B). The transcription of *Taz* (1.65-fold, $P = 0.0424$), *Pax7* (1.49-fold, $P = 0.0471$), *Myf5* (2.07-fold, $P = 0.0354$) and *Rheb1* (1.68-fold, $P = 0.0137$) was also increased in exercise-trained mice compared to control mice (Figure 6C). As expected, there was an increase in the number of Pax7⁺ cells/fibres after exercise (2.12-fold, 0.09 ± 0.02 vs. 0.20 ± 0.03 , $P = 0.0002$) (Figure 6D). The number of TAZ⁺ (2.01-fold, 14.12 ± 4.55 vs. 28.36 ± 5.61 ,

$P = 0.0038$) and Myf5⁺ (2.67-fold, 12.40 ± 4.53 vs. 33.12 ± 4.52 , $P = 0.0003$) cells among the Pax7⁺ cells was also increased after exercise (Figure 6E,F).

To investigate the effect of TAZ on exercise-mediated satellite cell activation, wt and sKO mice were examined after 4 weeks of exercise training. Muscle fibre diameter was reduced in sKO mice (0.76-fold, 61.07 ± 23.33 vs. 46.60 ± 24.29 μ m, $P = 0.0006$) compared to wt mice as shown in Figure 7A. Furthermore, sKO mice showed decreased levels of Pax7 (0.54-fold, $P = 0.0136$), Myf5 (0.63-fold, $P = 0.0318$) and cyclin D1 (0.50-fold, $P = 0.0104$) (Figure 7B). Decreased mTOR activity was also observed in sKO mice compared to

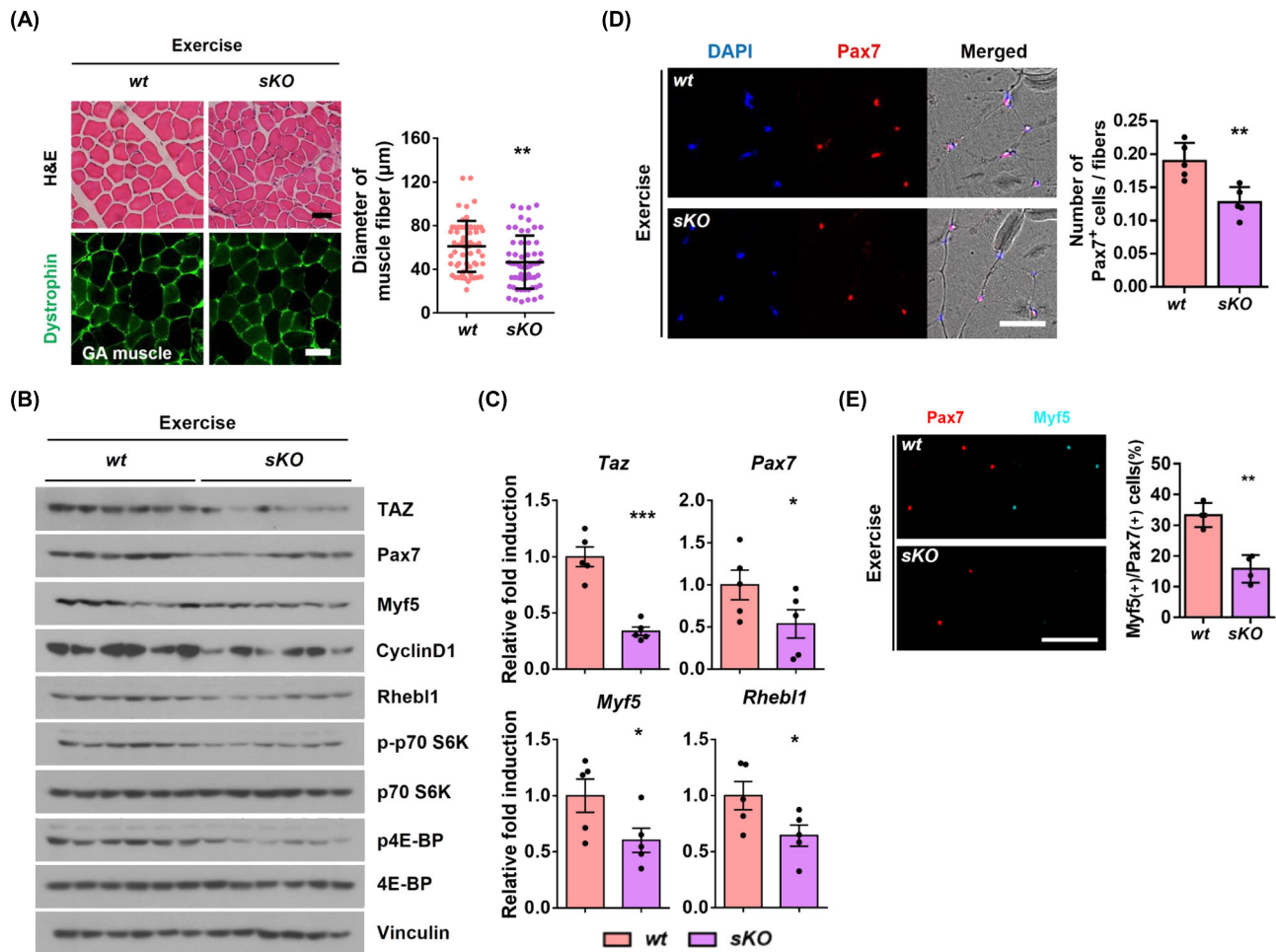


Figure 7 TAZ depletion in vivo reduces the number of satellite cells and myofiber diameter after exercise. (A) Wt and sKO mice were subjected to endurance exercise training. The GA muscles were harvested from these mice, and tissue immunostaining was performed. H&E and dystrophin (green) immunofluorescence staining of GA muscles from exercise-trained wt and sKO mice. Scale bar, 50 μ m. Muscle fiber diameters were quantified using ImageJ software. (B) TAZ, Pax7, Myf5, Cyclin D1, Rheb1, phospho-p70 S6K, p70 S6K, phospho-4E-BP, 4E-BP and Vinculin levels in GA muscles of exercise-trained wt and sKO mice were analysed by immunoblotting. (C) *Taz*, *Pax7*, *Myf5* and *Rheb1* transcript levels were analysed by qRT-PCR in GA muscles of exercise-trained wt and sKO mice ($n = 5$). (D) Immunofluorescence staining of Pax7 (red) in GA muscles of exercise-trained wt and sKO mice. Nuclei are stained with DAPI (blue). Scale bar, 50 μ m. The number of Pax7-positive cells was quantified relative to the number of fibres. (E) Immunofluorescence staining of Pax7 (red) and Myf5 (cyan) in GA muscles of exercise-trained wt and sKO mice. Scale bar, 50 μ m. The ratio of the number of Myf5-positive cells to the number of Pax7-positive cells was quantified. Data are presented as the mean \pm SEM. * $P < 0.05$, ** $P < 0.01$ and *** $P < 0.001$ (Student's t test).

wt mice as evidenced by decreased *Rheb1* (0.60-fold, $P = 0.0099$), p-p70 S6K (0.62-fold, $P = 0.0062$) and p-4E-BP (0.48-fold, $P = 0.0002$) (Figure 7B). The transcription of *Taz* (0.34-fold, $P = 0.0001$), *Pax7* (0.54-fold, $P = 0.0472$), *Myf5* (0.60-fold, $P = 0.0309$) and *Rheb1* (0.64-fold, $P = 0.0269$) was also decreased in sKO mice compared to wt mice (Figure 7C). The number of Pax7⁺ cells/fibres (0.61-fold, 0.20 ± 0.03 vs. 0.12 ± 0.02 , $P = 0.0013$) and Myf5⁺/Pax7⁺ cells (0.51-fold, 27.11 ± 4.24 vs. 13.73 ± 4.50 , $P = 0.0025$) was decreased in sKO mice compared to wt mice (Figure 7D,E). In conclusion, our study showed that TAZ stimulates muscle satellite cell activation and increases the number of satellite cells after exercise.

Discussion

Muscle satellite cells exit quiescence upon muscle injury and are activated to repair the muscle tissue. In this study, we showed that TAZ induced satellite cell activation for muscle regeneration after muscle injury and exercise (Figure 8). TAZ interacted with Pax7 and stimulated Myf5 expression to activate satellite cells, resulting in their myogenic differentiation. The physiological importance of TAZ in satellite cells was demonstrated in the muscles of sKO mice. TAZ depletion in Pax7⁺ satellite cells impaired satellite cell activation and muscle regeneration in sKO mice. TAZ and YAP are Hippo effectors that exhibit redundant biological functions,

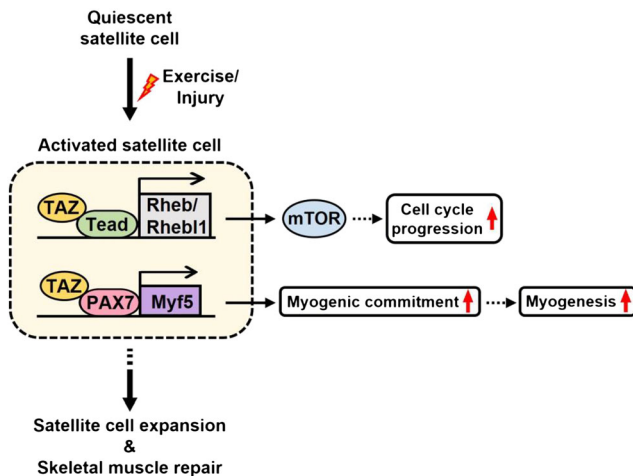


Figure 8 Proposed model. Quiescent satellite cells were activated by exercise or muscle injury. TAZ expression was upregulated in activated satellite cells, and the increased TAZ translocated to the nucleus and interacted with Pax7 and TEAD transcription factors. Myf5 transcription, which promotes the commitment of satellite cells to myogenic differentiation, was induced by Pax7 and TAZ interaction, and Rheb/Rheb1 transcription, which stimulates cell cycle progression by promoting mTOR signalling activation, was induced by TEAD and TAZ interaction. As a result, TAZ stimulates satellite cell expansion and promotes skeletal muscle repair.

including cell proliferation. Notably, we observed discrete functions of these proteins in satellite cell activation. YAP did not interact with Pax7 to induce Myf5 expression during satellite cell activation. These results suggest that TAZ and YAP have discrete roles in muscle regeneration due to preferential binding with transcription factors, including Pax7, and induction of their target genes. This result is in accordance with a previous study, which reported that in myogenic cells, TAZ and YAP promote the proliferation of myogenic cells, but TAZ, but not YAP, enhances myogenic differentiation.⁵⁵ Sun et al. have shown that both YAP and TAZ stimulate satellite cell-derived myoblast proliferation and that TAZ, not YAP, promotes satellite cell myogenesis.⁵¹¹ Sun et al. observed that active TAZ mutant (TAZS89A) stimulates myogenesis with induction of Myf5 and that the Myf5 induction was observed by TAZS89A, but not by active YAP mutant (YAPS127A).⁵¹¹ Silver et al. have also shown that depletion of YAP/TAZ reduces cell proliferation in C2C12 and that the effect is partially dominated by TAZ.⁵¹² Similar to their observation, we observed that satellite cell-specific TAZ KO mice show decreased satellite cell number and proliferation index (Figures 1D and S3). In addition, sKO mice show reduced regeneration activity (Figure 1E,F). Our study provides evidence for TAZ-induced myogenic differentiation during muscle regeneration.

mTORC1 activity is necessary for the transition of satellite cells from G_0 to G_{Alert} phase.¹⁶ Adult muscle stem

cell-specific mTORC1 deletion after injury significantly impaired muscle regeneration.¹⁹ Similarly, muscle satellite cell-specific deletion of p110 α , a catalytic subunit of phosphatidylinositol 3-kinase (PI3K), impaired the exit of satellite cell quiescence. This defect was partially rescued by genetic reactivation of mTORC1.⁵¹³ In addition, rapamycin, an mTOR inhibitor, limits age-related stem cell loss¹⁸ and restores the regenerative function of geriatric satellite cells.¹⁷ In accordance with previous reports, we observed that TAZ increased mitochondrial potential by stimulating mTOR activity in satellite cells (Figure 4). Recently, we reported that TAZ stimulates mitochondrial biogenesis in muscles through the activation of Rheb/Rheb1–mTOR signalling axis.⁵¹⁰ Indeed, TAZ depletion decreased mitochondrial potential and mTOR activity in satellite cells. These results suggest that the TAZ–mTOR signalling axis plays a critical role in satellite cell activation.

During muscle regeneration, the asymmetric division of satellite cells involves renewing satellite cells and committed cells into myocytes.^{20,514} During cell division, the polarity protein Pard3 is localized in committed cells attached to myofibres and activates p38 MAPK.²¹ The protein p38 α/β MAPK then functions as a molecular switch to activate quiescent satellite cells.⁵¹⁵ In satellite cell-specific p38 α knockout mice, p38 α restricts excess proliferation and promotes myogenic differentiation during the post-natal growth phase.⁵¹⁶ Indeed, the p38 MAPK signalling pathway regulates muscle stem cell fate decisions by inducing the expression of myogenic genes.^{517–519} In our study, TAZ was induced in committed cells, which was assessed by the activities of the polarity proteins, Pard3 and p38 MAPK (Figure 5). Thus, our study suggests that TAZ is a downstream effector of the p38 MAPK pathway and is activated in committed cells, thereby stimulating the transcription of myogenic marker genes for myogenic differentiation. In accordance with our study, another study showed Pard3-mediated TAZ stabilization in polarized epithelial cells.⁵²⁰

Endurance exercise training can improve muscle regeneration in old mice.^{31,32,521} Restoration of cyclin D1 is important for the rejuvenation of quiescent old satellite cells.³⁰ In our study, exercise increased TAZ level with cyclin D1 induction (Figure 6). This was impaired in sKO mice (Figure 7). These results suggest that TAZ may play an important role in the rejuvenation of quiescent satellite cells in old mice and may be an important target protein for the drug development in sarcopenia.

In conclusion, our study showed that TAZ stimulates satellite cell activation for muscle regeneration and that exercise-mediated TAZ induction facilitates muscle adaptation to exercise. This study suggests that activation of TAZ in satellite cells may ameliorate the ageing phenotype of muscle including reduced satellite cell number and its myogenic potential.

Acknowledgements

This work was supported by the National Research Foundation of Korea (NRF) funded by the Korean government (2021R1A2C1007461, 2020R1A2C2004679, 2018R1A5A2025286 and RS-2023-00221182) and Korea Drug Development Fund funded by Ministry of Science and ICT, Ministry of Trade, Industry and Energy, and Ministry of Health and Welfare (HN22C0723), Republic of Korea. This work was also supported by Korea Basic Science Institute (National Research Facilities and Equipment Center) grant funded by the Ministry of Education (2021R1A6C101A442) and a grant funded by Korea University.

Conflict of interest statement

The authors declare no competing interests.

Online supplementary material

Additional supporting information may be found online in the Supporting Information section at the end of the article.

References

- Chang NC, Rudnicki MA. Satellite cells: the architects of skeletal muscle. *Curr Top Dev Biol* 2014;**107**:161–181.
- Wang YX, Rudnicki MA. Satellite cells, the engines of muscle repair. *Nat Rev Mol Cell Biol* 2011;**13**:127–133.
- Bischoff R, Heintz C. Enhancement of skeletal muscle regeneration. *Dev Dyn* 1994;**201**:41–54.
- Rudnicki MA, Schnegelsberg PN, Stead RH, Braun T, Arnold HH, Jaenisch R. MyoD or Myf-5 is required for the formation of skeletal muscle. *Cell* 1993;**75**:1351–1359.
- Cornelison DD, Wold BJ. Single-cell analysis of regulatory gene expression in quiescent and activated mouse skeletal muscle satellite cells. *Dev Biol* 1997;**191**:270–283.
- Cooper RN, Tajbakhsh S, Mouly V, Cossu G, Buckingham M, Butler-Browne GS. In vivo satellite cell activation via Myf5 and MyoD in regenerating mouse skeletal muscle. *J Cell Sci* 1999;**112**:2895–2901.
- Kadi F, Charifi N, Denis C, Lexell J, Andersen JL, Schjerling P, et al. The behaviour of satellite cells in response to exercise: what have we learned from human studies? *Pflugers Archiv: Eur J Physiol* 2005;**451**:319–327.
- Yin H, Price F, Rudnicki MA. Satellite cells and the muscle stem cell niche. *Physiol Rev* 2013;**93**:23–67.
- Sacco A, Doyonnas R, Kraft P, Vitorovic S, Blau HM. Self-renewal and expansion of single transplanted muscle stem cells. *Nature* 2008;**456**:502–506.
- Zammit PS, Golding JP, Nagata Y, Hudon V, Partridge TA, Beauchamp JR. Muscle satellite cells adopt divergent fates: a mechanism for self-renewal? *J Cell Biol* 2004;**166**:347–357.
- Collins CA, Olsen I, Zammit PS, Heslop L, Petrie A, Partridge TA, et al. Stem cell function, self-renewal, and behavioral heterogeneity of cells from the adult muscle satellite cell niche. *Cell* 2005;**122**:289–301.
- Blau HM, Cosgrove BD, Ho AT. The central role of muscle stem cells in regenerative failure with aging. *Nat Med* 2015;**21**:854–862.
- Sousa-Victor P, Garcia-Prat L, Serrano AL, Perdiguero E, Munoz-Canoves P. Muscle stem cell aging: regulation and rejuvenation. *Trends Endocrinol Metab* 2015;**26**:287–296.
- Laplante M, Sabatini DM. mTOR signaling in growth control and disease. *Cell* 2012;**149**:274–293.
- Laplante M, Sabatini DM. Regulation of mTORC1 and its impact on gene expression at a glance. *J Cell Sci* 2013;**126**:1713–1719.
- Rodgers JT, King KY, Brett JO, Cromie MJ, Charville GW, Maguire KK, et al. mTORC1 controls the adaptive transition of quiescent stem cells from G₀ to G_{Alert}. *Nature* 2014;**510**:393–396.
- Garcia-Prat L, Martínez-Vicente M, Perdiguero E, Ortet L, Rodríguez-Ubreva J, Rebollo E, et al. Autophagy maintains stemness by preventing senescence. *Nature* 2016;**529**:37–42.
- Haller S, Kapuria S, Riley RR, O'Leary MN, Schreiber KH, Andersen JK, et al. mTORC1 activation during repeated regeneration impairs somatic stem cell maintenance. *Cell Stem Cell* 2017;**21**:806–818.e5.
- Rion N, Castets P, Lin S, Enderle L, Reinhard JR, Eickhorst C, et al. mTOR controls embryonic and adult myogenesis via mTORC1. *Development* 2019;**146**:dev172460.
- Dumont NA, Bentzinger CF, Sincennes MC, Rudnicki MA. Satellite cells and skeletal muscle regeneration. *Compr Physiol* 2015;**5**:1027–1059.
- Troy A, Cadwallader AB, Fedorov Y, Tyner K, Tanaka KK, Olwin BB. Coordination of satellite cell activation and self-renewal by Par-complex-dependent asymmetric activation of p38 α / β MAPK. *Cell Stem Cell* 2012;**11**:541–553.
- Chen W, Datzkiw D, Rudnicki MA. Satellite cells in ageing: use it or lose it. *Open Biol* 2020;**10**:200048.
- Murach KA, Fry CS, Dupont-Versteegden EE, McCarthy JJ, Peterson CA. Fusion and beyond: satellite cell contributions to loading-induced skeletal muscle adaptation. *FASEB J* 2021;**35**:e21893.
- Kadi F, Schjerling P, Andersen LL, Charifi N, Madsen JL, Christensen LR, et al. The effects of heavy resistance training and detraining on satellite cells in human skeletal muscles. *J Physiol* 2004;**558**:1005–1012.
- Mackey AL, Esmarck B, Kadi F, Koskinen SO, Kongsgaard M, Sylvestersen A, et al. Enhanced satellite cell proliferation with resistance training in elderly men and women. *Scand J Med Sci Sports* 2007;**17**:34–42.
- Petrella JK, Kim JS, Mayhew DL, Cross JM, Bamman MM. Potent myofiber hypertrophy during resistance training in humans is associated with satellite cell-mediated myonuclear addition: a cluster analysis. *J Appl Physiol* 2008;**104**:1736–1742.
- Mackey AL, Andersen LL, Frandsen U, Sjogaard G. Strength training increases the size of the satellite cell pool in type I and II fibres of chronically painful trapezius muscle in females. *J Physiol* 2011;**589**:5503–5515.
- Kurosaka M, Naito H, Ogura Y, Machida S, Katamoto S. Satellite cell pool enhancement in rat plantaris muscle by endurance training depends on intensity rather than duration. *Acta Physiol (Oxf)* 2012;**205**:159–166.
- Shefer G, Rauner G, Stuelsatz P, Benayahu D, Yablonka-Reuveni Z. Moderate-intensity treadmill running promotes expansion of the satellite cell pool in young and old mice. *FEBS J* 2013;**280**:4063–4073.
- Brett JO, Arjona M, Ikeda M, Quarta M, de Morrée A, Egner IM, et al. Exercise rejuvenates quiescent skeletal muscle stem cells in old mice through restoration of Cyclin D1. *Nat Metab* 2020;**2**:307–317.
- Shefer G, Rauner G, Yablonka-Reuveni Z, Benayahu D. Reduced satellite cell numbers and myogenic capacity in aging can be alleviated by endurance exercise. *PLoS ONE* 2010;**5**:e13307.
- Joanisse S, Nederveen JP, Baker JM, Snijders T, Iacono C, Parise G. Exercise conditioning in old mice improves skeletal muscle regeneration. *FASEB J* 2016;**30**:3256–3268.

33. Yu FX, Zhao B, Guan KL. Hippo pathway in organ size control, tissue homeostasis, and cancer. *Cell* 2015;**163**:811–828.
34. Meng Z, Moroishi T, Guan KL. Mechanisms of Hippo pathway regulation. *Genes Dev* 2016;**30**:1–17.
35. Piccolo S, Dupont S, Cordenonsi M. The biology of YAP/TAZ: Hippo signaling and beyond. *Physiol Rev* 2014;**94**:1287–1312.
36. Barry ER, Camargo FD. The Hippo superhighway: signaling crossroads converging on the Hippo/Yap pathway in stem cells and development. *Curr Opin Cell Biol* 2013;**25**:247–253.
37. Cai J, Zhang N, Zheng Y, de Wilde RF, Maitra A, Pan D. The Hippo signaling pathway restricts the oncogenic potential of an intestinal regeneration program. *Genes Dev* 2010;**24**:2383–2388.
38. Barry ER, Morikawa T, Butler BL, Shrestha K, de la Rosa R, Yan KS, et al. Restriction of intestinal stem cell expansion and the regenerative response by YAP. *Nature* 2013;**493**:106–110.
39. Gregorieff A, Liu Y, Inanlou MR, Khomchuk Y, Wrana JL. Yap-dependent reprogramming of Lgr5⁺ stem cells drives intestinal regeneration and cancer. *Nature* 2015;**526**:715–718.
40. Byun MR, Hwang JH, Kim AR, Kim KM, Park JI, Oh HT, et al. SRC activates TAZ for intestinal tumorigenesis and regeneration. *Cancer Lett* 2017;**410**:32–40.